The highly expressed ERV1 forms virus-like particles for regulating early embryonic development

Authors: Wenjing Li[1,3†], Shujuan Liu[1,3†], Jianglin Zhao[1†], Ruizhi Deng[1†], Yayi Liu[1], Huijia Li[1], Hongwei Ma[1], Yanzhi Chen[1], Jingcheng Zhang[1], Yongsheng Wang[1], Jianmin Su[1], Fusheng Quan[1], Xu liu[2*],Yan Luo[2*], Yong Zhang[1*], and Jun Liu[1*]

Affiliations:

1 College of Veterinary Medicine, Northwest A&F University, Key Laboratory of Animal Biotechnology of the Ministry of Agriculture, Yangling 712100, Shaanxi, China.

2 Department of Animal Engineering, Yangling Vocational and Technical College, Yangling 712100, China.

3 Reproductive hospital, Jiangxi University of Traditional Chinese Medicine, Nanchang 330004, Jiangxi, China.

† Contributed equally to this work

* Corresponding author. Tel: (+86) 029-87011230, E-mail address: yl_ly2019@163.com (Yan Luo). Tel: (+86) 029-87080085, E-mail address: zhy1956@263.net (Yong Zhang). Tel: (+86) 029-87080092, E-mail address: liujun2013@nwsuaf.edu.cn (Jun Liu).

Running title: ERV1 essential for early embryonic development

Abstract

In mammals, the transcription of transposable elements (TEs) is important for maintaining early embryonic development. Here, we systematically analyzed the expression characteristics of TE-derived transcripts in early embryos by constructing a database of TEs and transcriptome data from goats and using it to study the function of endogenous retroviruses (ERVs) in regulating early embryo development. We found that ERV1 made up the highest proportion of TE sequences and exhibited a stage-specific expression pattern during early embryonic development. Among ERV elements, ERV1 had the potential to encode the Gag protein domain to form virus-like particles (VLPs) in early goat embryos. Knockdown of ERV1_1_574 significantly reduced the embryo development rate and the number of trophoblast cells ($P< 0.05$). Transcriptome sequencing analysis of morula embryos showed that ERV1_1_574 mainly regulated the expression of genes related to embryo compaction and trophoblast cell differentiation, such as CX43 and CDX2. In summary, we found that ERV1 expression was essential for early embryonic development in goats through regulation of trophoblast cell differentiation.

Keywords: transposable elements; endogenous retrovirus; virus-like particles; trophoblast cell differentiation; transcriptome sequences; embryonic development

Introduction

TEs are mobile genomic DNA sequences, which are ubiquitous to all organisms and are an important part of the host genome. In humans (44%), mice (40%), cattle (46%) and other organisms, TEs account for almost half of the host genome (Lander *et al*, 2001; Waterston *et al*, 2002; Adelson *et al*, 2009), and increasing evidence indicates that TEs have important effects on the structure, function and evolutionary dynamics of the genome (Xu & Wang, 2007; Rho & Tang, 2009; Senft & Macfarlan, 2021). Recent studies have reported that a large number of transcripts of TEs have been discovered at specific stages of early embryonic development, but their biological functions and regulatory mechanisms have not been fully determined (Gifford *et al*, 2013; Fu *et al*, 2019).

Whole-genome sequencing revealed high variability in the number, type, and sequence of TEs despite the high sequence homology of functional genes in mammals (Platt *et al*, 2018). At present, the TE sequences of a variety of animals can be retrieved from the Repbase database, but the sequences of TEs in the goat genome have not been included or reported yet. Determining the functions and regulatory mechanisms of TEs in early embryonic development of domestic animals is the key to revealing their characteristics in early embryo development. Studies have demonstrated that LINE1 (Beraldi *et al*, 2006), MuERV-L (Kigami *et al*, 2003), LincGET (Wang *et al*, 2018) and HPAT5 (Durruthy-Durruthy *et al*, 2016), among others, are essential regulatory elements for maintaining early embryonic development.

ERV elements constitute a large part of the TEs in eukaryotic genomes (Makalowski *et al*, 2012), accounting for about ten percent of the mammalian genome (Rebollo *et al*, 2012), and many studies showed that ERVs were important for regulating mammalian gene expression (Friedli & Trono, 2015; Thompson *et al*, 2016). Genes of the mouse endogenous retrovirus-like (MERVL) virus initiate a large number of specific transcripts at the two-cell embryo stage (Kigami *et al*, 2003; Macfarlan *et al*, 2012). For example, the ERV-related lncRNA, LincGET, is indispensable for cell division in mouse embryos (Wang *et al*, 2016). In some ERVs, the Gag sequence has

the capacity to encode proteins, and the Gag protein forms VLPs that can infect and transmit information between cells, thus performing a regulatory and communication function. In two-cell stage mouse embryos, some MERVL virus sequences can also encode Gag protein (Macfarlan *et al*, 2012). During Drosophila oogenesis, ERV elements in trophoblasts express VLPs, which can infect oocytes and may regulate oogenesis (Wang *et al*, 2018). Many mammalian ERV element transcripts have been discovered in early embryos, but the mechanism of their regulation of embryo development needs further clarification.

In our previous study, we found that ERV-derived lncRNAs affect the development rate of early goat embryo blastocysts by regulating the expression of the target gene, CHD1L (Deng *et al*, 2019). In this study, a database of TEs in the goat genome was established, and the transcriptome of early goat embryos at various stages was generated by RNA-seq. We systematically analyzed the transcripts of TEs in early goat embryos, and focused on the expression and function of ERV1. We found that ERV1_1_574 was highly expressed in goats during early embryonic development and could encode Gag protein and form virus-like particles. Moreover, ERV1_1_574 could affect embryo development by regulating embryo densification.

Results

ERVs are the largest superfamily of TEs in the goat genome

We obtained the sequences of all TEs in the goat genome based on de novo prediction, structure-based prediction and homology-based prediction strategies **(Fig. S1)**. We classified and annotated the TEs to build a comprehensive, user-friendly, web-based database (http://genedenovoweb.ticp.net:81/goatTEdb/) **(Fig.S2)**. A total of 495,065 TEs from 21 super-families and 926 families were included in this database **(Table 1)**. The coverage and classification of TEs in the goat genome were determined by RepeatMasker. We found that the percentage of the goat genome consisting of TEs was similar to that of cattle at 46.33%. LINEs accounted for 10.31% of the genome, which was lower than for cattle (23.29%), humans (20.40%) and mice (19.59%). SINEs made up 2.86% of the goat genome, compared to 17.66% for cattle, 13.11%

for humans, and 7.34% for mice. ERVs constituted 28.45% of the goat genome, which was significantly higher than that of cattle (3.20%), humans (8.56%) and mice (9.84%). ERV1 had the highest copy number (12,366 members) among all subclasses in the goat genome **(Table 2)**. The goat TEs were evenly distributed in every chromosome except chromosome 10 **(Fig. S3A)**. Using the sequences of the intact elements to construct a maximum likelihood tree, we identified one BovB, 91 L1, and 41 ERV1 active elements **(Fig. S3B)**. The high proportion of ERVs revealed by TE analysis was a significant feature of the goat genome, in which the ERV1 copy number was particularly high and contained a large proportion of active elements.

Transcriptome analysis of early goat embryos using RNA-seq

We collected in vitro fertilized (IVF) early goat embryos at various stages **(Fig. 1A)**, and used RNA-seq technology to obtain the transcriptomes. We aligned the reads to the goat genome and assembled the transcripts to analyze mRNA and potential lncRNA expression in early goat embryos **(Fig. S1, Table 3)**. Principal component analysis (PCA) showed that the different developmental stages of embryos could be separated into distinct groups based on gene counts **(Fig. S4)**. The total expression levels of mRNAs and lncRNAs in 8-cell stage embryos were increased during early embryonic development **(Fig. 1B)**. Large-scale transcriptional activation occurred at the 8-cell stage, as expected for embryonic genome activation (EGA) of early goat embryos. The heatmap of dynamic gene expression showed that differentially expressed genes (DEGs) in 8-cell embryos and morula embryos were different from the zygote, 2-cell and 4-cell stage embryos **(Fig. 1C)**. To further explore the dynamic expression patterns of DEGs, we divided all developmental stages into three modules **(Fig. 1D)**. The first module included up-regulated genes in zygotic, 2-cell and 4-cell stages. These were defined as maternal genes and a total of 41 were identified, including 15 lncRNAs and 26 mRNAs, which were enriched in cell division, cell cycle, mitosis, and mitotic cell cycle G/2M transitions. The second module contained highly expressed genes in 8-cell stage embryos. There were 51 genes in total, including 25 lncRNAs and 26 mRNAs. Notably, the typical ZSCAN4

zygotically-activated genes in mice and humans were in this module. GO enrichment indicated that genes in the second module were related to protein binding, DNA binding regulation and GTPase activation. The third module included highly co-expressed genes of 8-cell stage and morula embryos, and 28 genes were screened, including 12 lncRNAs and 16 mRNAs. Genes were mainly enriched for transcription factor activity, transcriptional regulation and transcription-related entries. The second and third modules were collectively defined as zygotic genes, mainly related to transcriptional and regulatory pathways.

ERV1 exhibits a highly expressed, stage-specific pattern in early goat embryos

ERVs were the most abundant class of TE in the goat genome in comparison with bovine, human and mouse genomes **(Table 2, Fig. 2A)**. The expression pattern of TE-derived transcripts in the transcriptome data from each developmental stage of early goat embryos was analyzed **(Fig. S1)**. We found that ERV1s accounted for the highest proportion in the transcriptome at all stages (the top six TEs expressed) **(Fig. 2B)**. Moreover, the number of specifically expressed ERV1s significantly increased in the 8-cell stage embryos when focusing on the ERV1, RTE, and L1 specifically expressed in embryos at different developmental stages ($P< 0.01$) **(Fig. 2C)**. We aligned transcriptome sequences with TE databases to obtain dynamic expression levels of transcripts associated with transposon elements. PCA **(Fig. S5A**) and dynamic expression analysis of all screened stage-specific elements showed that the TEs (ERV1, L1 and RTE) were stage-specifically expressed during development of early goat embryos **(Fig. 2D and S5A)**. We selected the representative maternal gene expression element ERV1_1_2471 and the zygotic gene expression element ERV1_1_12704 for IGV visualization **(Fig. S5B)**, and the sequencing data were verified by RT-qPCR **(Fig. S5C)**. These findings suggested that ERV1s were highly expressed in early goat embryos and exhibited stage-specific expression patterns.

ERV1 has the potential to form virus-like particles (VLPs)

We performed structural predictions on all ERV1s with complete ERV sequences

(domains > 2), and found structures typical of overlapping Gag, Pro and Pol genes in the RNA coding region of ERV1 sequences **(Fig. S6)**. We found that the gag protein structures of ERV1_1_574 and ERV1_1_1613 had the potential to encode a virus-like capsid Gag protein domain P10, P24 and P30 that may generate VLPs **(Fig. 3A)**. The expression level of candidate ERV1 in early embryos was verified by RT-qPCR, and ERV1_1_574 and ERV1_1_1613 were highly expressed at the eight-cell stage **(Fig. 3B)**.

TEM results revealed a large number of VLPs distributed in the spaces between blastomeres and in the perivitelline space **(Fig. 4A)**. After ERV1_1_574 knockdown, we found that the number of VLPs was significantly decreased both in the space between blastomeres **(Fig. 4B)** and in the perivitelline space **(Fig. 4C)** in 8-cell stage embryos ($P< 0.01$). These results showed that ERV1_1_574 encoded the Gag protein domain to form VLPs in goat early embryos.

ERV1_1_574 is necessary for early embryo development

We performed RNAi experiments to verify how ERV1 affected early embryonic development **(Fig. 5A)**. The results showed that silencing of ERV1_1_574 significantly reduced the blastocyst development rate, while knockdown of ERV1_1_1613 had no significant effect on embryonic development **(Fig. 5B and C)**. Interestingly, we found that the densification of morula in the ERV1_1_574 knockdown group was significantly affected **(Fig. 5D)**, and few embryos developed beyond sixteen cells to the morula or blastocyst stage **(Fig. 5E and F)**. We performed blastocyst quality assessment experiments through CDX2 staining and found that the total number of blastocyst cells and the number of trophoblast cells in the knockdown group were significantly reduced ($P<0.05$), but the number of inner cell masses was not significantly different **(Fig. 6A and B)**. The apoptotic staining experiments revealed that apoptotic cell numbers in blastocysts were significantly increased in the knock-down group relative to the controls ($P<0.001$) **(Fig. 6C and D)**.

ERV1_1_574 regulated embryo compaction and trophoblast

differentiation-related genes

To elucidate the mechanism of ERV1_1_574's effect on embryo development at the gene level, we performed transcriptome sequencing analysis of morula embryos and obtained 351 differentially expressed transcripts **(Fig.7A)**, of which 188 were upregulated and 163 were downregulated **(Fig. 7B)**. KEGG analysis **(Fig.7C)** and GO enrichment analysis **(Fig.7D)** showed that differential genes were enriched in cell adhesion, cell junction and other pathways. RT-qPCR was used to validate the expression levels of the DEGs, CX43 (a connexin-encoding gene) and CDX2 (embryo lineage differentiation gene), associated with embryo compaction and trophoblast differentiation. Knockdown of ERV1_1_574 significantly decreased the expression of CX43 and CDX2 in morulas **(Fig.7E)**. These results indicated that ERV1_1_574 affected embryonic development by regulating the expression of embryo compaction and trophoblast differentiation-related genes.

Discussion

ERVs constitute a large number of TE elements in eukaryotic genomes (Mager & Stoye, 2015). Systematic elucidation of the expression and function of ERV elements is useful for revealing the regulatory mechanism of early embryonic development (Gifford *et al*, 2013; Friedli & Trono, 2015; Hutchins & Pei, 2015). In this study, we constructed a TE database and comprehensively analyzed the expression patterns of ERVs during early goat embryo development. We screened ERV1 for its potential to encode a gag protein and detected the presence of VLPs in goat embryos. We found that ERV1_1_574 knockdown caused the arrest of embryos mostly at the 8- to16-cell stage; therefore, we explored the possible biological function of ERV1_1_574 on early embryonic development in goats.

The subfamily and function of reactivated ERV elements in early embryos were different among mammal species. In mouse, MuERV-L was an important marker of zygotic genome activation with important functions in early embryo development and establishment of pluripotency (Kigami *et al*, 2003; Macfarlan *et al*, 2012). In early human embryos, HERVH was mainly expressed in the inner cell mass and promoted

embryonic stem cells through the encoded lncRNA, HPAT5 (Durruthy-Durruthy *et al*, 2016; Wang *et al*, 2016). ERV1s were highly expressed in early embryos, but their function and regulation were unclear in bovines (Bui *et al*, 2009). Our results showed that ERV1_1_574 was highly expressed specifically during EGA, and that ERV1_1_574 knockdown significantly reduced embryo compaction and trophoblast differentiation in goats.

ERV elements were involved in regulating gene expression during embryonic development through various pathways, including promoter/enhancer activity, non-coding RNA (lncRNA), functional proteins, and epigenetic modification (Chuong *et al*, 2017; Hendrickson *et al*, 2017). In previous studies, HERV-K LTR was shown to contain multiple transcriptional start sites (TSS), and alternate TSS were part of the active regulation of gene transcription directed by LTRs (Fuchs *et al*, 2011; Persson *et al*, 2016). The ERV-derived lncRNA, LincGET, influenced inner cell mass (ICM) development and induced cell fate decisions (Wang *et al*, 2018). The HERV-W env protein acted as a fusion protein to promote the formation of syncytiotrophoblast cells (Frendo *et al*, 2003). HERV-K, which exists in repressed chromatin regions, has a strong association with H3K9me3 and is able to both activate and suppress gene expression (Campos-Sánchez *et al*, 2016). Our study found that ERV1_1_574 affected the development of early embryos by regulating the expression of CX43 and CDX2, which are genes related to embryo compaction and trophoblast differentiation. We also determined whether ERV-encoded Gag protein could regulate embryonic development.

In recent years, the functions and regulatory mechanisms of various ERV-derived non-coding RNAs have been unraveled (Gerdes *et al*, 2016); however, less is known about the function and regulation of Gag proteins encoded by complete ERV sequences. Previous studies revealed that the complete ERV element, MuERV-L, could produce Gag protein and form VLPs in 2-cell stage mouse embryos (Macfarlan *et al*, 2012). In addition, the envelope protein of endogenous Jaagsiekte sheep retrovirus (enJSRVs) was able to regulate trophectoderm growth and differentiation in peri-implantation embryos (Dunlap *et al*, 2006). Here, we confirmed the presence of

Gag protein VLPs in early goat embryos, and established that ERV1_1_574, had the ability to express Gag protein, and significantly affect the rate of embryo development, and the rate and quality of blastocyst formation. Whether ERV1_1_574 regulated this process alone, or through Gag proteins, is still under investigation.

The Gag proteins produced by ERVs have specific biological functions in placental development. The Fv1 (Friend virus susceptibility-1) gene, encoded by the mouse MuERV-L Gag protein gene, can limit infection by the mouse leukemia virus MuLVs (Sanz-Ramos & Stoye, 2013). In sheep, the Gag protein encoded by enJSRV restricted the replication of exogenous viruses by blocking their interaction with receptors (Arnaud *et al*, 2007). Recent studies have shown that VLPs derived from ERVs can enclose their own RNAs and transmit them between cells, suggesting that virus particles derived from ERVs are capable of mediating cell communication. During Drosophila oogenesis, transposons were passed from supporting nurse cells to eggs by means of microtubules to promote oocyte development, proving that transposons can be passed from cell to cell (Wang *et al*, 2018). In neurons, the Arc gene encodes a Gag-like protein that forms VLPs, and the Arc gene mRNA is delivered to other neuronal cells in the form of exosomes (Pastuzyn *et al*, 2018). Additional studies will need to be done to determine whether the Gag protein encoded by ERV1 can be assembled into VLPs that can act like exosomes to encapsulate specific RNAs and pass through the cytomembrane in early goat embryos to mediate communication between blastomeres.

In summary, our study demonstrated that ERV1 had the potential to encode the Gag protein domain to form VLPs that regulate trophoblast cell differentiation in early goat embryos. Although only a subset of ERVs has been studied during early embryonic development, our findings highlight the unexplored functions of ERVs in regulating embryonic development.

Materials and Methods

Establishment of goat TE database

According to the latest goat genome data, LAMP (Linux Ubuntu Server 12.04, Apache 2, MySQL Server 5.5, Perl 5.16.3/ PHP 5.3) was used to construct a database of TEs from the goat genome. The TE data were stored as MySQL tables. Common gateway interface (CGI) programs were adapted using Perl, JavaScript and PHP programming languages. The JBrowse genome browser is an embedded genome browser produced with HTML5 and JavaScript that was employed to manipulate and depict the positional relationships between genes and TEs in the goat database (Skinner et al., 2009). The establishment of the goat TE database was mainly based on the signature, homology, and Denove methods. Predict LTRs (long terminal repeats), Helitron MITEs (miniature inverted repeat transposable elements), LINEs (long interspersed nuclear elements), SINEs (short interspersed nuclear elements), and TIRs (terminal inverted repeats) were identified. The filter sequence was redundant, and the filter criterion was identity >90%. LTRs and LINEs were used for superfamily identification by direct comparison with the Repbase database, and family identification was based on the 80-80-80 principle for classification. The coverage and classification of transposon elements in the goat genome was performed using RepeatMasker (http://www.repeatmasker.org, v 4.0.3). The Repbase update collection was down-loaded from http://www.girinst. org/repbase/index.html (Jurka et al., 2005). The position of the transposon sequence in the genome was obtained by using the visualization software from UCSC. The Jukes-Cantor step-length was calculated and the appearance of the evolutionary tree was further edited by Mega v7 (Kumar et al., 2016). Lastly, the potential active elements in the open reading frame were identified via CLC sequence Viewer 5 (CLC Bio). The data used in this study was down-loaded from the goat genome database https://www.ncbi.nlm.nih.gov/genome/?term=goat.

Goat embryo collection and culture

The goat ovaries were collected from an abattoir, placed in saline containing 100 U/ml penicillin/ streptomycin at 20℃, and transported to the lab within six hours. The organs were washed 3× and incubated in TCM-199 (Gibco-BRL, NY, US) with 25

mM HEPES, 10% fetal bovine serum, and 2 IU/mL heparin. Follicles (2-6 mm diameter) were removed, and cumulus-cell oocyte complexes (COCs) with intact/dense cumulus cells were removed under a stereo-microscope. After washing with phosphate-buffered saline, 100 COCs were pipetted into four-well plates and cultured in maturation medium (TCM-199 supplemented with 10% FBS, 0.2 mM sodium pyruvate, 0.075 IU/mL human menopausal gonadotropin, 1 μg/mL 17β-estradiol, 10 ng/mL epidermal GF, and 1% insulin/transferrin-selenium) for about 24 hours at 38°C in a CO_2 incubator.

Commercial cryopreserved semen (SKXing Breeding Biotechnology, Inner Mongolia, China) was employed for fertilization. Fifty microliter sperm aliquots (2×10^6 sperm/mL) were incubated with 40 to 50 COCs in 400 μL BO-IVF medium (IVF Bioscience, Falmouth, UK). After twelve hours, the COCs were removed and the zygotes transferred into 400 μL BO-IVC medium (IVF Bioscience, Falmouth, UK) and layered with mineral oil. Embryos were removed at specific stages for experiments.

RNA-seq

The single-cell RNA-seq technology (SUPeR-seq) developed by Tang et al. was performed to profile the whole transcriptome (Fan et al., 2015). Briefly, the three best quality embryos at each developmental stage were disrupted in single-cell sequencing lysis buffer (blastocysts were not used to construct the sequencing library for technical reasons). RNA was reverse transcribed into cDNA using the T15N6 primers from the SuperScript III kit. The amplified and purified cDNA product was sheared into 150-350 bp fragments by Covaris S2. Fragmented DNA was amplified using the TruSeq DNA library building kit. All libraries were sequenced on an Illumina platform to generate the raw data. Approximately 11.4 million reads were obtained per sample.

The sequencing data were filtered with SOAPnuke (v1.5.2) (Li et al., 2008), and clean reads were mapped to the goat assembly ARS1 genome using HISAT2 (v2.0.4) (Kim et al., 2015). Transcripts were assembled by StringTie (Pertea et al., 2015) to generate

novel, known transcripts. Fragments per gene were counted using HTSeq-count (version 0.12.4) (PMID: 25260700) from aligned reads. Fragments per kb of exon model per million mapped fragments (FPKM) were determined using DESeq2 (v1.4.5) (Love et al., 2014) after data normalization. To compare expression of genes between different developmental stages, normalization of reads coverage and differential gene expression analysis at the different developmental stages were performed using DEseq2. The threshold of differential expressed genes was $P< 0.05$, |fold change| > 1.

Analysis of the source transcripts of TEs

Protein-based RepeatMasking in Repeatmasker was used to compare the transcriptome sequence with all transposon element libraries and obtain dynamic expression levels of transcripts related to transposon elements.

Predictive analysis of ERV1 domains

GenomeTools 1.5.7 was used to analyze the structure of ERV1 and to predict the structure of ERV1 with domains >3.

RT-qPCR

Embryos at the zygotic, two-, four-, and eight-cell stages, and morulae were harvested, respectively, at 1, 2, 3, and 5 days after fertilization or activation on day 0. The PrimeScript™ RT reagent kit with gDNA eraser (Takara) was used to convert total RNA to cDNA. SYBR® Premix Ex Taq™ II and a one-step real-time PCR system (Applied Biosystems) was used to do reverse-transcription quantitative PCR (RT-qPCR). The primer sequences are shown in Table 3, and data are compared as fold-change = $2^{-\Delta\Delta Ct}$ means ± SD.

Embryonic RNA interference (RNAi)

The siRNA against the sheep ERV1_1_574 transcript was created and synthesized by GenePharma (Shanghai, China) (Table 4). The siRNA was aliquotted at 20 μM and kept at □80°C. About 10 pL of siRNA was injected into a presumed fertilized egg

(collected 20 hours after IVF). The siRNA was microinjected under a microscope (Axio Observer D1, Zeiss) equipped with a micro-manipulation device (TransferMan NK2, Eppendorf) and a micro-injector (FemtoJet, Eppendorf). A volume of 1μL of siRNA was drawn from the bottom of the tube through a micro-sampler (Eppendorf). During microinjection, the embryo was inside a 100 μL droplet of M199/HEPES (Gibco) plus 10% fetal bovine serum.

Differential staining and apoptosis analysis of early embryonic cells

Experimentally treated blastocysts and control blastocysts were collected on day 7, fixed with 4% paraformaldehyde at room temperature for 4 hours, and permeabilized with 0.1% Triton X-100 at room temperature for 20 minutes. The blastocysts were blocked in immunostaining blocking medium at 4°C overnight followed by incubation with anti-CDX2 (BioGenex Inc., US) at 4°C overnight. After washing, the blastocysts were incubated with AlexaFluor 555-conjugated donkey anti-mouse IgG for 2 h in the dark at room temperature. After washing again, the nuclei in the samples were stained with DAPI (Beyotime, China) and the stained cells were imaged under a fluorescence microscope. The total number of blastocyst cells, trophoblast cells and inner cell clusters were counted.

Another group of blastocysts was collected for measuring apoptosis. After fixing and permeabilization, the blastocysts were transferred to a solution of 45 μL of E-buffer, 5 μL dNTP Nad mix, and 1μL rTdT, and incubated at 37°C in the dark for 1 hour. Reactions were terminated by addition of 2X SSC, nuclei were stained with DAPI, and apoptosis was observed under a fluorescence microscope. The total number of blastocyst cells (DAPI) and apoptotic cells (FITC) were counted and the apoptosis rate was determined. The TUNEL assay kit used in the experiment was from Promega Corporation.

Transmission electron microscopy

Eight-cell stage embryos were fixed with 2.5% glutaraldehyde for 1 hour at 4°C. The agar embedding method was used to embed 30-40 embryos in a 2 mm x 2 mm x 2

mm agar block. The agar blocks were rinsed three times with 0.1 M phosphate buffer, fixed with 1% osmic acid solution for 2-4 h, then dehydrated twice in graded ethanol solutions: 30%, 50%, 70%, 80%, 90%, and 100%. Samples in 100% ethanol were immersed in LR-White embedding agent (3:1) for 2 h, 1:1 for 8h, 1:3 for 12 h, and lastly, 100% LR-White for 24 h, overnight. The samples were placed in the embedding polymerizer for automatic polymerization and then sectioned, first as semi-thin sections and, after positioning, as ultra-thin sections. The ultra-thin sections were floated onto copper meshes, stained with uranyl acetate, then with lead citrate, dried naturally and observed under a transmission electron microscope.

Analysis of ERV1 expression interference by embryonic gene expression

Heatmaps of the various samples were constructed using P-heatmap (v1.0.8) based on gene-expression profiles. Differential expression was determined using DESeq2 (v1.4.5) (Fan et al., 2015) with q value ≤ 0.05. For additional insights into the changes of phenotypes, GO (http://www.geneontology.org/) and KEGG (https://www.kegg.jp/) enrichment analysis of annotated DEGs was done using the P-hyper package (https://en.wikipedia.org/wiki/Hypergeometric_distribution) based on the hypergeometric test. The significance levels of terms and pathways were corrected according to q values with a strict threshold of q≤ 0.05, using the Bonferroni test.

Statistical analysis

Appropriate statistics tests were performed using SPSS 22.0 (SPSS Inc., US). Experiments were repeated at least three times, and data are means ± standard error of the mean (SEM). For RT-qPCR, the value of $2^{-\triangle\triangle Ct}$ was measured to compare the relative gene expression of experimental with control groups. Student's *t* test or Chi-squared test was used for paired comparison, and one-way analysis of variance was done for multiple comparisons. P< 0.05 indicated significance

Compliance and ethics

All animal procedures and experiments were conducted in accordance with the Guide for the Care and Use of Laboratory Animals (Ministry of Science and Technology of China, 2006), and were approved by the animal ethics committee of Northwest A&F University.

Acknowledgments

We thank Ronghua Zhang for providing the goat ovaries.

Author contributions

Wenjing Li: Data curation, Methodology, Formal analysis, Writing. Shujuan Liu: Methodology, Formal analysis. Jianglin Zhao: Methodology, Formal analysis. Ruizhi Deng: Methodology, Formal analysis. Yayi Liu: Methodology, Resources. Huijia Li: Methodology, Resources. Hongwei Ma: Methodology, Resources. Yanzhi Chen: Writing. Jingcheng Zhang: Methodology, Resources. Yongsheng Wang: Methodology, Resources. Jianmin Su: Methodology, Resources. Fusheng Quan: Methodology, Resources. Yong Zhang: Project administration, Xu liu and Yan Luo: Conceptualization. Jun Liu: Conceptualization, Writing, Funding acquisition.

Competing interests

The authors declare that they have no conflict of interest.

References

Adelson DL, Raison JM, Edgar RC (2009) Characterization and distribution of retrotransposons and simple sequence repeats in the bovine genome. Proc Natl Acad Sci U S A 106: 12855-12860

Arnaud F, Murcia PR, Palmarini M (2007) Mechanisms of late restriction induced by an endogenous retrovirus. J Virol 81: 11441-11451

Beraldi R, Pittoggi C, Sciamanna I, Mattei E, Spadafora C (2006) Expression of LINE-1 retroposons is essential for murine preimplantation development. Mol Reprod Dev 73: 279-287

459 Bui LC, Evsikov AV, Khan DR, Archilla C, Peynot N, Hénaut A, Le Bourhis D,
460 Vignon X, Renard JP, Duranthon V (2009) Retrotransposon expression as a defining
461 event of genome reprograming in fertilized and cloned bovine embryos. Reproduction
462 138: 289-299
463 Campos-Sánchez R, Cremona MA, Pini A, Chiaromonte F, Makova KD (2016)
464 Integration and fixation preferences of human and mouse endogenous retroviruses
465 uncovered with functional data analysis. Plos Comput Biol 12: e1004956
466 Chuong EB, Elde NC, Feschotte C (2017) Regulatory activities of transposable
467 elements: From conflicts to benefits. Nat Rev Genet 18: 71-86
468 Deng R, Han C, Zhao L, Zhang Q, Yan B, Cheng R, Wei B, Meng P, Mao T, Zhang Y
469 et al (2019) Identification and characterization of ERV transcripts in goat embryos.
470 Reproduction 157: 115-126
471 Dunlap KA, Palmarini M, Varela M, Burghardt RC, Hayashi K, Farmer JL, Spencer
472 TE (2006) Endogenous retroviruses regulate periimplantation placental growth and
473 differentiation. Proc Natl Acad Sci U S A 103: 14390-14395
474 Durruthy-Durruthy J, Sebastiano V, Wossidlo M, Cepeda D, Cui J, Grow EJ, Davila J,
475 Mall M, Wong WH, Wysocka J et al (2016) The primate-specific noncoding RNA
476 HPAT5 regulates pluripotency during human preimplantation development and
477 nuclear reprogramming. Nat Genet 48: 44-52
478 Frendo JL, Olivier D, Cheynet V, Blond JL, Bouton O, Vidaud M, Rabreau M,
479 Evain-Brion D, Mallet F (2003) Direct involvement of HERV-W Env glycoprotein in
480 human trophoblast cell fusion and differentiation. Mol Cell Biol 23: 3566-3574
481 Friedli M, Trono D (2015) The developmental control of transposable elements and
482 the evolution of higher species. Annu Rev Cell Dev Bi 31: 429-451
483 Fu B, Ma H, Liu D (2019) Endogenous retroviruses function as gene expression
484 regulatory elements during mammalian pre-implantation embryo development. Int J
485 Mol Sci 20: 790
486 Fuchs NV, Kraft M, Tondera C, Hanschmann KM, Lower J, Lower R (2011)
487 Expression of the human endogenous retrovirus (HERV) group HML-2/HERV-K does
488 not depend on canonical promoter elements but is regulated by transcription factors

sp1 and sp3. J Virol 85: 3436-3448

Gerdes P, Richardson SR, Mager DL, Faulkner GJ (2016) Transposable elements in the mammalian embryo: Pioneers surviving through stealth and service. Genome Biol 17: 100

Gifford WD, Pfaff SL, Macfarlan TS (2013) Transposable elements as genetic regulatory substrates in early development. Trends Cell Biol 23: 218-226

Hendrickson PG, Dorais JA, Grow EJ, Whiddon JL, Lim JW, Wike CL, Weaver BD, Pflueger C, Emery BR, Wilcox AL et al (2017) Conserved roles of mouse DUX and human DUX4 in activating cleavage-stage genes and MERVL/HERVL retrotransposons. Nat Genet 49: 925-934

Hutchins AP, Pei D (2015) Transposable elements at the center of the crossroads between embryogenesis, embryonic stem cells, reprogramming, and long non-coding RNAs. Sci Bull 60: 1722-1733

Kigami D, Minami N, Takayama H, Imai H (2003) MuERV-L is one of the earliest transcribed genes in mouse One-Cell embryos1. Biol Reprod 68: 651-654

Lander ES, Linton LM, Birren B, Nusbaum C, Zody MC, Baldwin J, Devon K, Dewar K, Doyle M, Fitzhugh W et al (2001) Initial sequencing and analysis of the human genome. Nature 409: 860-921

Macfarlan TS, Gifford WD, Driscoll S, Lettieri K, Rowe HM, Bonanomi D, Firth A, Singer O, Trono D, Pfaff SL (2012) Embryonic stem cell potency fluctuates with endogenous retrovirus activity. Nature 487: 57-63

Mager DL, Stoye JP (2015) Mammalian endogenous retroviruses. Microbiol Spectr 3: A3-A9

Makalowski W, Pande A, Gotea V, Makalowska I (2012) Transposable elements and their identification. Methods Mol Biol 855: 337-359

Pastuzyn ED, Day CE, Kearns RB, Kyrke-Smith M, Taibi AV, Mccormick J, Yoder N, Belnap DM, Erlendsson S, Morado DR et al (2018) The neuronal gene arc encodes a repurposed retrotransposon gag protein that mediates intercellular RNA transfer. Cell 172: 275-288

Persson J, Steglich B, Smialowska A, Boyd M, Bornholdt J, Andersson R, Schurra C,

519 Arcangioli B, Sandelin A, Nielsen O et al (2016) Regulating retrotransposon activity
520 through the use of alternative transcription start sites. Embo Rep 17: 753-768
521 Platt RN, Vandewege MW, Ray DA (2018) Mammalian transposable elements and
522 their impacts on genome evolution. Chromosome Res 26: 25-43
523 Rebollo R, Romanish MT, Mager DL (2012) Transposable elements: An abundant and
524 natural source of regulatory sequences for host genes. Annu Rev Genet 46: 21-42
525 Rho M, Tang H (2009) MGEScan-non-LTR: Computational identification and
526 classification of autonomous non-LTR retrotransposons in eukaryotic genomes.
527 Nucleic Acids Res 37: e143
528 Sanz-Ramos M, Stoye JP (2013) Capsid-binding retrovirus restriction factors:
529 Discovery, restriction specificity and implications for the development of novel
530 therapeutics. J Gen Virol 94: 2587-2598
531 Senft AD, Macfarlan TS (2021) Transposable elements shape the evolution of
532 mammalian development. Nat Rev Genet 22: 691-711
533 Thompson PJ, Macfarlan TS, Lorincz MC (2016) Long terminal repeats: From
534 parasitic elements to building blocks of the transcriptional regulatory repertoire. Mol
535 Cell 62: 766-776
536 Wang J, Li X, Wang L, Li J, Zhao Y, Bou G, Li Y, Jiao G, Shen X, Wei R et al (2016)
537 A novel long intergenic noncoding RNA indispensable for the cleavage of mouse
538 two-cell embryos. Embo Rep 17: 1452-1470
539 Wang J, Singh M, Sun C, Besser D, Prigione A, Ivics Z, Hurst LD, Izsvák Z (2016)
540 Isolation and cultivation of naive-like human pluripotent stem cells based on HERVH
541 expression. Nat Protoc 11: 327-346
542 Wang J, Wang L, Feng G, Wang Y, Li Y, Li X, Liu C, Jiao G, Huang C, Shi J et al
543 (2018) Asymmetric expression of LincGET biases cell fate in Two-Cell mouse
544 embryos. Cell 175: 1887-1901
545 Wang L, Dou K, Moon S, Tan FJ, Zhang ZZ (2018) Hijacking oogenesis enables
546 massive propagation of LINE and retroviral transposons. Cell 174: 1082-1094
547 Waterston RH, Lindblad-Toh K, Birney E, Rogers J, Abril JF, Agarwal P, Agarwala R,
548 Ainscough R, Alexandersson M, An P et al (2002) Initial sequencing and comparative

549 analysis of the mouse genome. Nature 420: 520-562

550 Xu Z, Wang H (2007) LTR_FINDER: An efficient tool for the prediction of

551 full-length LTR retrotransposons. Nucleic Acids Res 35: W265-W268

552

553 **Figure legends**

554

555 **Figure 1** Transcriptome dynamics in early goat embryos

556 **(A)** Microscopy images of goat pre-implantation embryos at zygote, two-, four-, and
557 eight-cell stages, morulae and blastocysts. Scale bar=20 μm. **(B)** The mRNA and
558 lncRNA expression patterns during goat preimplantation development. **(C)**
559 Hierarchical clustering analysis shows stage-specific (|fold change| >2, $P< 0.05$)
560 expression of genes in goat preimplantation embryo samples. Differentially-expressed
561 genes (DEGs) were appropriately aggregated into different clusters. Red: high
562 expression. Blue: low expression. **(D)** Cluster analysis of DEGs. Clusters of DEGs by
563 normalized FPKM reflect the total transcript content per sample during
564 preimplantation development. All of the genes shown were differentially expressed
565 between two consecutive stages (|fold change| >2, $P< 0.05$). The DEGs can be
566 classified as follows: (1) 42 maternal genes with two to three clusters activated in the
567 8-cell stage defined as zygotic genes; (2) 51 zygotic genes, and (3) 29 zygotic genes.
568 The expression level is shown in the middle panel and GO enrichment is shown in the
569 right panel.

570

571 **Figure 2** ERV1 is a specific element in goat TE-derived transcripts

572 **(A)** The proportion of TEs in genomes of different species. **(B)** Relative abundance of
573 TEs at different developmental stages. Relative abundance of transcripts were derived
574 from the first six classes of repetitive elements at the indicated stages. **(C)** The
575 number of ERV1s, RTEs and L1s specifically expressed at different stages compared
576 to other stages. **(D)** Dynamic expression of ERV1, L1 and RTE elements at different
577 stages.

578

579 **Figure 3** ERV1 has the potential to encode the Gag protein viral capsid

580 **(A)** ERV1_1_574 and ERV1_1_1613 have Gag and LTR structures at both ends,
581 where Gag_P24 is the core capsid protein. **(B)** Quantitative PCR (qPCR) analysis of
582 ERV1_1_574 and ERV1_1_1613 expression levels in in vitro-fertilized embryos at

583 various stages. Error bars indicate SEM.

584

585 **Figure 4** There are a large number of ERV1-derived virus-like particles in early
586 embryos

587 **(A)** Electron micrographs of Gag particles from the 8-cell stage of goat embryos.
588 Virions appear mainly in the blastomere space and between the blastomere and the
589 zona pellucida. Arrows: Gag particles; stars: zona pellucida. Scale bar: 200 nm. **(B)**
590 The number of Gag particles in the blastomere space. Error bars, SEM. ***P*<0.01. **(C)**
591 Number of Gag particles in the gap between blastomere and zona pellucida. Error bars,
592 SEM. ***P*<0.01.

593

594 **Figure 5** Knockdown of ERV1_1_574 affects early embryonic development
595 **(A)** Expression of ERV1_1_574 and ERV1_1_1613 at the 8- to 16-cell stage of IVF
596 embryos developed from siRNA/C-injected zygotes. Error bars = SEM. **P*< 0.05,
597 ***P*< 0.01. **(B)** Representative images of control embryos and those siRNA-injected
598 as blastocysts. Scale bar = 100 μm. **(C)** Development rate of the cleavage and
599 blastocysts in siRNA/C-injected embryos. Error bars = SEM. **P*< 0.05; ***P*< 0.01.
600 **(D)** Degree and morphology of morula densification in siRNA/C-injected embryos.
601 Scale bar = 20 μm. **(E)** Development rate of cleavage, 8- to16-cell stage, morula and
602 blastocysts in embryos. Error bars = SEM. **P*< 0.05; ** *P*< 0.01. **(F)** Developmental
603 embryonic progression after siRNA/C injections. χ^2 P values were calculated for the
604 developmental rate of embryos injected with siRNA.

605

606 **Figure 6** Knockdown of ERV1_1_574 affects blastocyst quality
607 **(A)** Staining for CDX2 (*red*) and DAPI (*blue*) in blastocysts developing from
608 siRNA/C-injected zygotes. Scale bar = 15 μm. **(B)** Box plots show total cell numbers,
609 TE cell numbers and ICM cell numbers of goat blastocysts from siRNA/C-injected
610 zygotes. **P*< 0.05 (Student's *t* test). **(C)** Apoptotic cells (*green*) showing nuclei (*blue*)
611 of blastocysts developing from siRNA/C-injected zygotes. Scale bar = 15 μm. **(D)**
612 Box plots indicate the apoptotic cell number (TUNEL-positive) of goat blastocysts

613 from the siRNA/C-injected zygotes. ***P*<0.01 (Student's *t* test).

614

615 **Figure 7** Influence of ERV1_1_574 on embryo densification is related to gap-junction
616 protein
617 **(A)** Hierarchical clustering analysis of 351 differentially expressed lncRNAs and
618 mRNAs between the control group and the knockdown group at the morula stage.
619 Data are from FPKM. Red: high expression. Blue: low expression. **(B)** Compared
620 with the knockdown group, 188 genes were upregulated and 163 genes were
621 downregulated in the control group. **(C)** KEGG pathway terms are displayed for 351
622 DEGs in morulae of IVF embryos following siRNA/C microinjections. **(D)** GO
623 analysis of DEGs in morulae of IVF embryos following siRNA/C microinjections. **(E)**
624 Expression of CX43 and CDX2 in morulae of in vitro-fertilized embryos developed
625 from siRNA/C-injected zygotes. Error bars indicate SEM. ***P*< 0.01.

626

627 **Tables legends**

628

629 Table 1 The TEs identified in the goat genome
630 Table 2 Proportion of TEs in goat genome compared with cattle, human and mouse
631 Table 3 Number of mRNAs and lncRNAs in goat transcriptome
632 Table 4 siRNA sequences for RNA interference
633 Table 5 Primer sequences for RT-qPCR
634

635 **Supplementary Data Legends**

636

637 **Figure S1** Flow chart of TE-derived transcripts

638 Left: flow chart of complete TEs. A total of 495,065 complete TEs were identified

639 based on three methods (*ab initio* prediction, structure prediction and homology

640 prediction strategy). All TEs were classified into 21 superfamilies by comparing the

641 custom repeat library with the Repbase. According to the 80-80-80 rule, all putative

642 goat TEs were classified into 926 families. Right: lncRNA and mRNA discovery for

643 RNA-Seq. Bottom, TE-derived transcripts. We used Blastall to blast lncRNA and

644 mRNA with complete TEs.

645

646 **Figure S2** User interface for browsing in GOAT-TEdb

647 **(A)** Menu of GOAT-TEdb. **(B-D)** Browsing interface of database GOAT-TEdb.

648

649 **Figure S3** Chromosomal distribution and maximum likelihood trees of TEs

650 **(A)** Location of goat TEs in the genome. The x axis corresponds to the chromosomes,

651 the y axis to nucleotide coordinates in million base-pairs (Mbp) in the goat genome.

652 **(B)** Intact RTE , L1 and ERV trees. Maximum likelihood trees derived from global

653 alignments of all intact/full-length LINEs and ERV sequences. Red lines depict

654 potentially active LINEs or ERVs based on their ORF content.

655

656 **Figure S4** Sample correlation analysis

657 **(A)** Correlation of single-cell goat sequencing samples. Principal-component analysis

658 of the transcriptomes of single embryos during preimplantation development. **(B)**

659 Pearson correlation-coefficient heatmap of single embryo transcriptomes during

660 preimplantation development.

661

662 **Figure S5**. Stage-specific TE expression during early goat embryonic development

663 **(A)** PCA of ERV1, LINE1 and RTE expression estimates in pre-implantation goat

664 embryos. The TEs showing the largest variation between the stages were chosen.

665 ERV1, LINE1and RTE expression are representative of the different development
666 stages. (B) Normalized RNA-seq for two loci showing stage-specific ERV1
667 expression (ERV1_1_2471 and ERV1_1_12704). (C) Expression profile of
668 ERV1_1_2471 and ERV1_1_12704. β-actin was used as a control. Error bars = SEM.
669
670 **Figure S6** Structural features of ERV sequences
671 Gag, Pol and Pro indicate ERV repeat regions.
672

673 **Table 1 The TEs identified in the goat genome**

Class	Order	Super-family	Member no.	Family no.
Retrotransposons	SINE	SINE	461,901	56
	LTR	Copia	127	5
		DIRS	14	13
		ERV1	12,366	8
		ERV4	1	1
		ERVK	3,332	6
		ERVL	272	46
		Gypsy	1,816	49
		Pao	187	6
	LINE	CR1	5	5
		I	3	1
		L1	835	12
		L2	3	3
		RTE	2,179	1
DNA transposons	TIR	CMC	1	1
		hAT	171	165
		PIF-Harbinger	5	5
		TcMar	113	100
		Unknown	9,256	166
	MITE	MITE	15	15
	Helitron	Helitron	2463	262
Total			495,065	926

674

675 **Table 2 Proportion of TEs in goat genome compared with cattle, human and**
676 **mouse**

Group	No.	Total bp	Capra hircus%	Bos taurus%	Human%	Mouse%
Non-LTR retrotransposons (LINEs)						
L1	835	44,127,212	1.50975	11.26352	17.07	19.14
RTE (BovB)	2179	257,153,877	8.79816	10.74072	NA	0.02
L2	3	30,383	0.00104	1.18416	3.07	0.37
CR1	5	74,331	0.00254	0.10569	0.27	0.06
Total	3022	301,385,803	10.31149	23.29409	20.40	19.59
SINEs	461901	83,495,632	2.85669	17.66441	13.11	7.34
BOVA	78	17,751	0.0006	14.2722	NA	NA
MIR	1	169	0.00	1.39034	2.43	0.05
other	13	1,277	0.00	0.01482	10.68	6.78
tRNA	461809	83,476,435	2.856	1.98705	NA	0.00
ERVs	16880	831,540,291	28.44999	3.19961	8.56	9.84
DNA transposons	2794	86,201,828	2.94928	1.95882	3.00	0.89
LTR other	2149	301,385,803	1.75835	0.42480	0.00	0.01
Interspersed repeat total	486746	1,604,009,357	46.3258	46.54174	45.08	37.65

677

678 **Table 3 Number of mRNAs and lncRNAs in goat transcriptome**

Group name	Known mRNA Num	New mRNA Num	All mRNA Num	Known lncRNA Num	New lncRNA Num	All lncRNA Num
Zygote	12,407	6,895	19,302	247	1,862	2,109
2cell	13,701	7,380	21,081	291	2,239	2,530
4cell	15,444	7,912	23,356	355	2,596	2,951
8cell	10,934	5,775	16,709	234	1,103	1,337
Morula	13,246	6,366	19,612	357	1,094	1,451

679

680

681 **Table 4 siRNA sequences for RNA interference**

Gene	Sequence (5′–3′)
β-actin-F	CTGGGACGACATGGAGAAGATC
β-actin-R	GCAGGGGTGTTGAAGGTCTC
ERV1_1_574-F	GCAGAGGTGGAGCAGAAGGTT
ERV1_1_574-R	CAGATGAGGCGGAATTAGACGA
ERV1_1_1613-F	GCTTTCTAGTCGCACGATACCA
ERV1_1_1613-R	GGCTTTAACCCTCACAGTCTTGTT
CX43_F	TTGGAGGTGGTACTCAACAGC
CX43_R	TGGACCACCTAATGCAACCTT
CDX2_F	GGAACCTGTGCGAGTGGATG
CDX2_R	TCTGCGGTTCTGAAACCAAAT

682

683

684 **Table 5 Primer sequences for RT-qPCR**

siRNA ID	Target sequences
ERV1_1_574-siRNA1	GGGUCCAAUAUCAGCACAATT
ERV1_1_574-siRNA2	CCGUAUUGUGAGCAAGCAATT
ERV1_1_574-siRNA3	GGUUCCGGAUCAGGAACAUTT
ERV1_1_1613-siRNA1	GGACAUUCUUUGGCCCAAUTT
ERV1_1_1613-siRNA2	GCGCAAUUGGCACUCCUUUTT
ERV1_1_1613-siRNA3	GGCCAAUAUUGAUGAGUUUTT

685

686 **Fig.1**

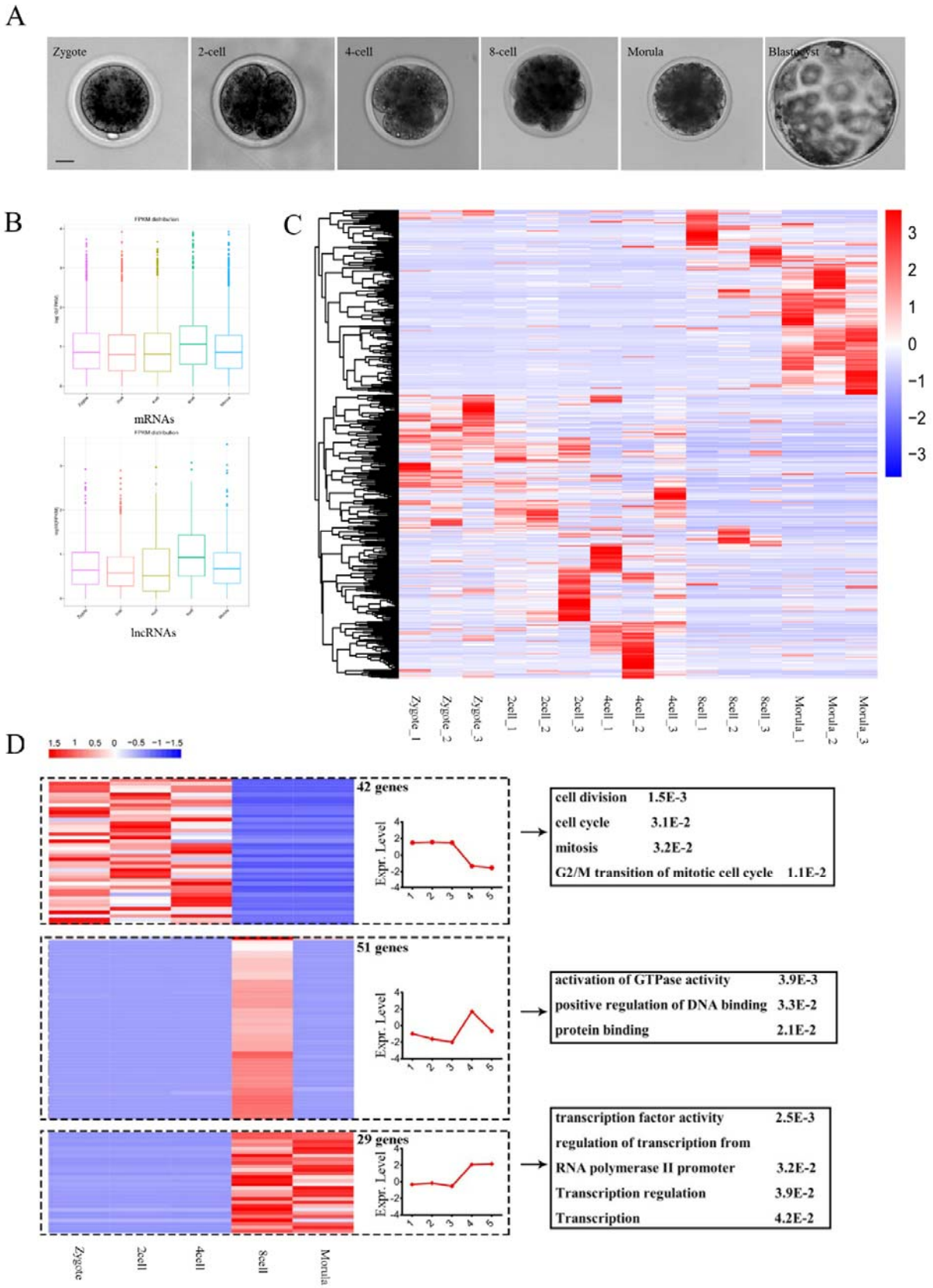

687 **Fig.2**

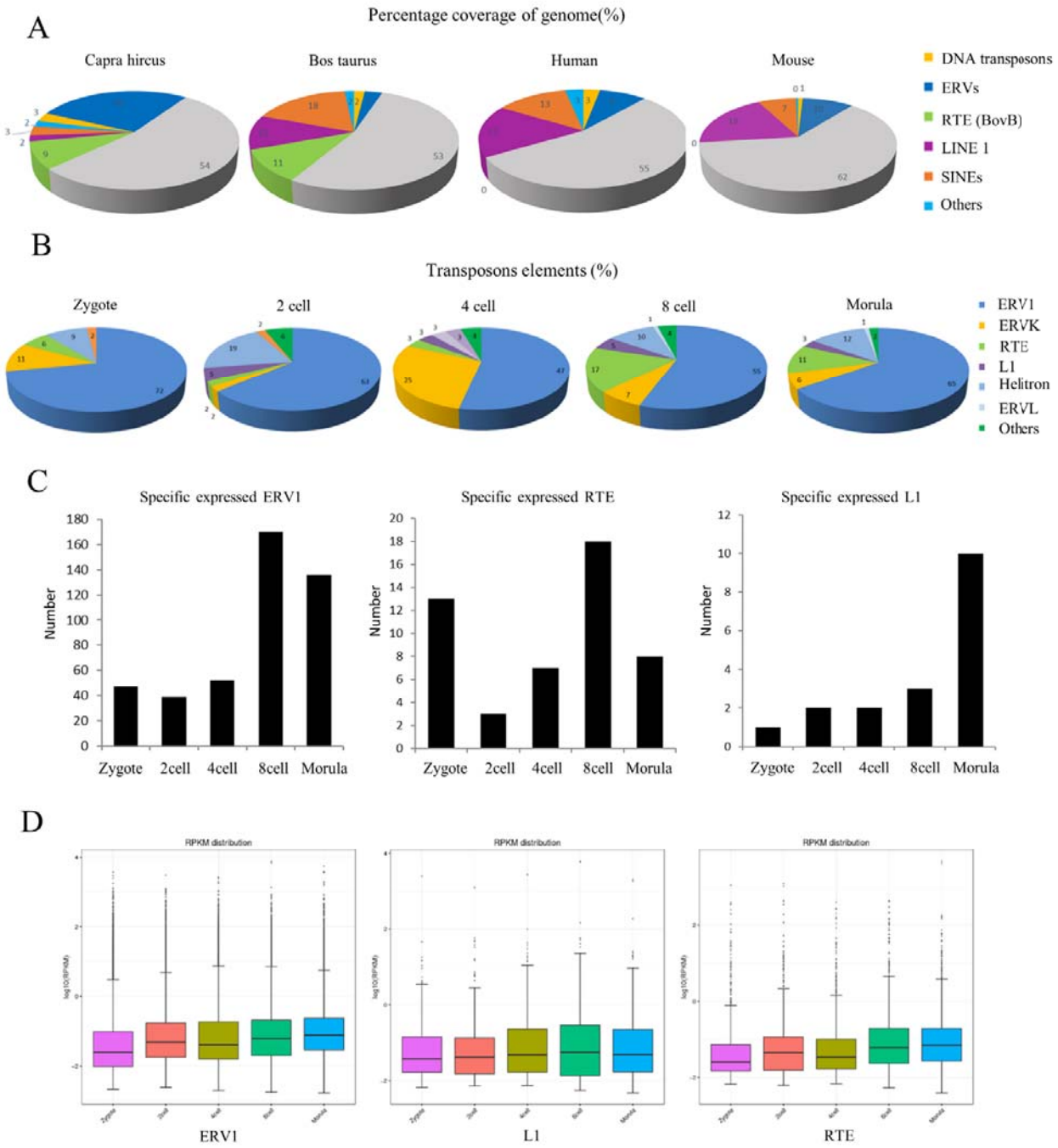

688

689 **Fig.3**

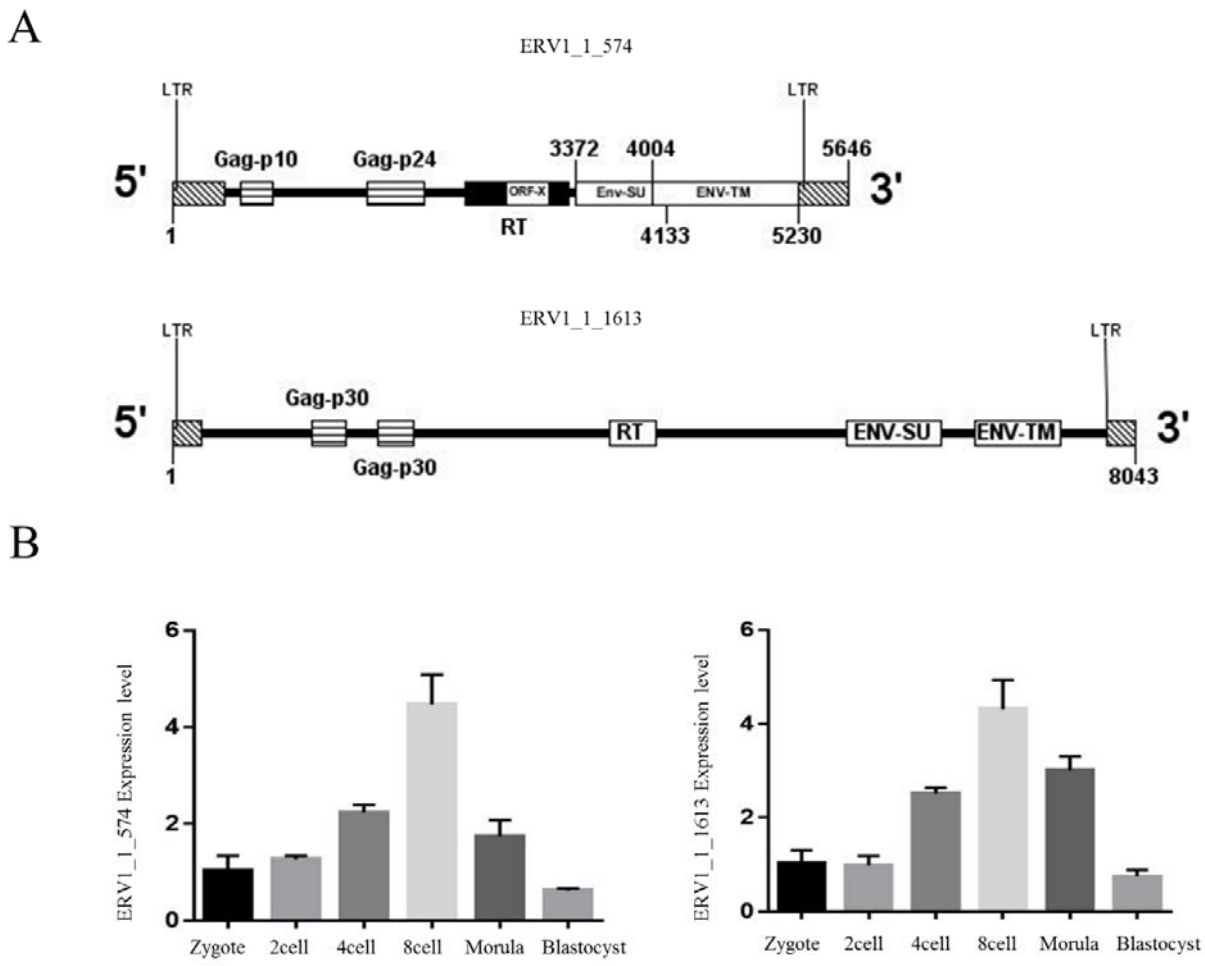

690

691 **Fig.4**

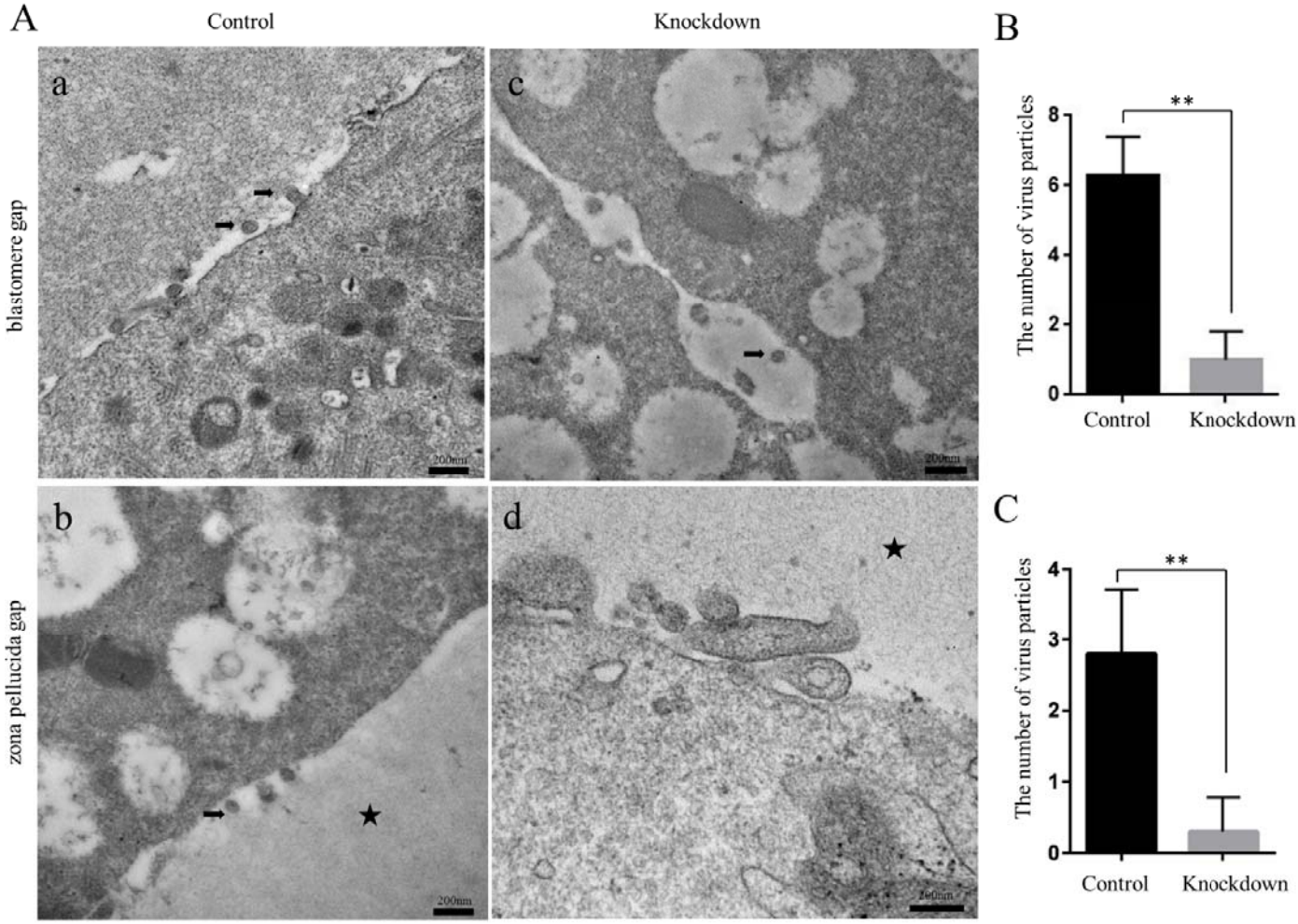

692

693 **Fig.5**

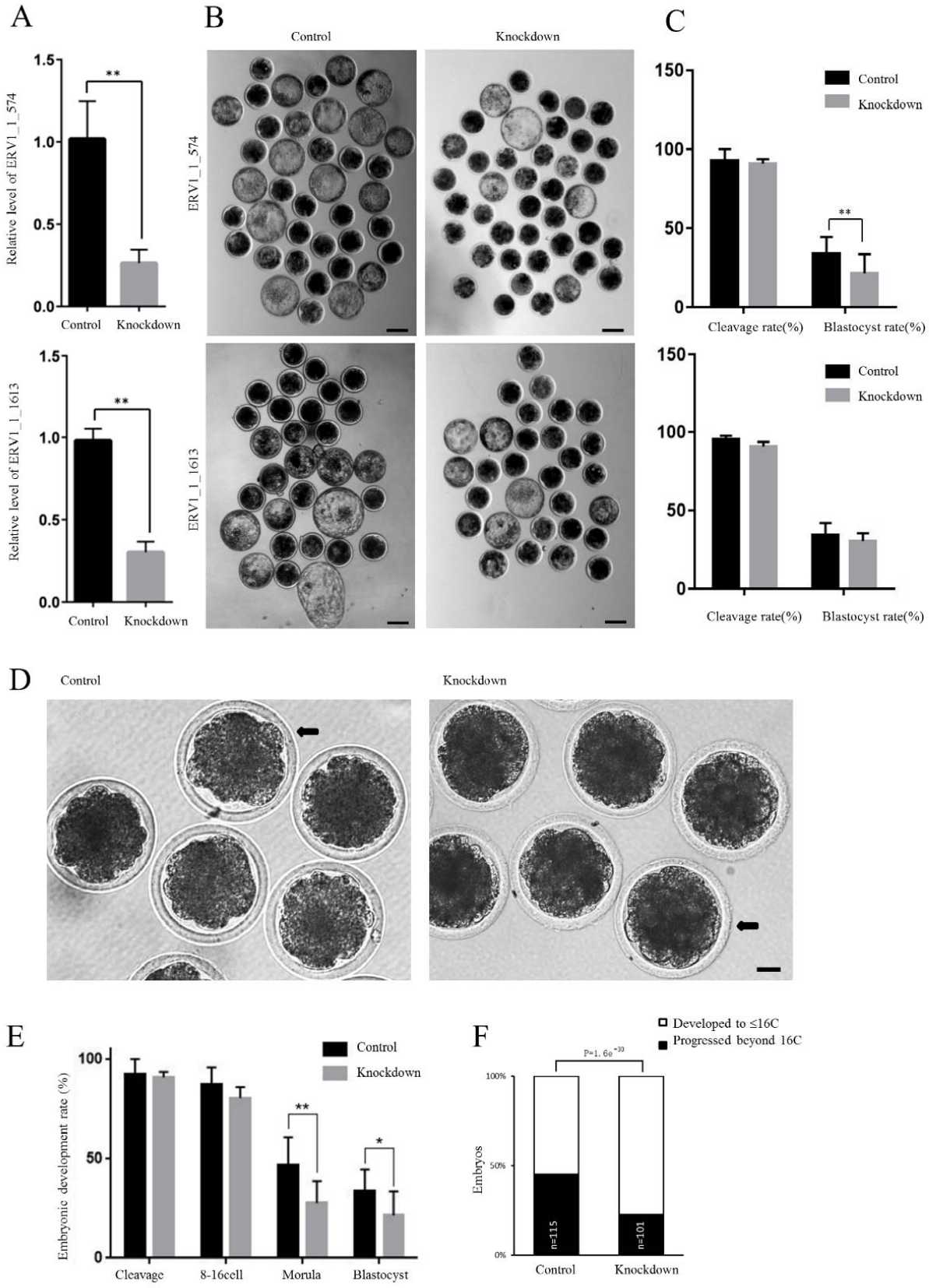

694 **Fig.6**

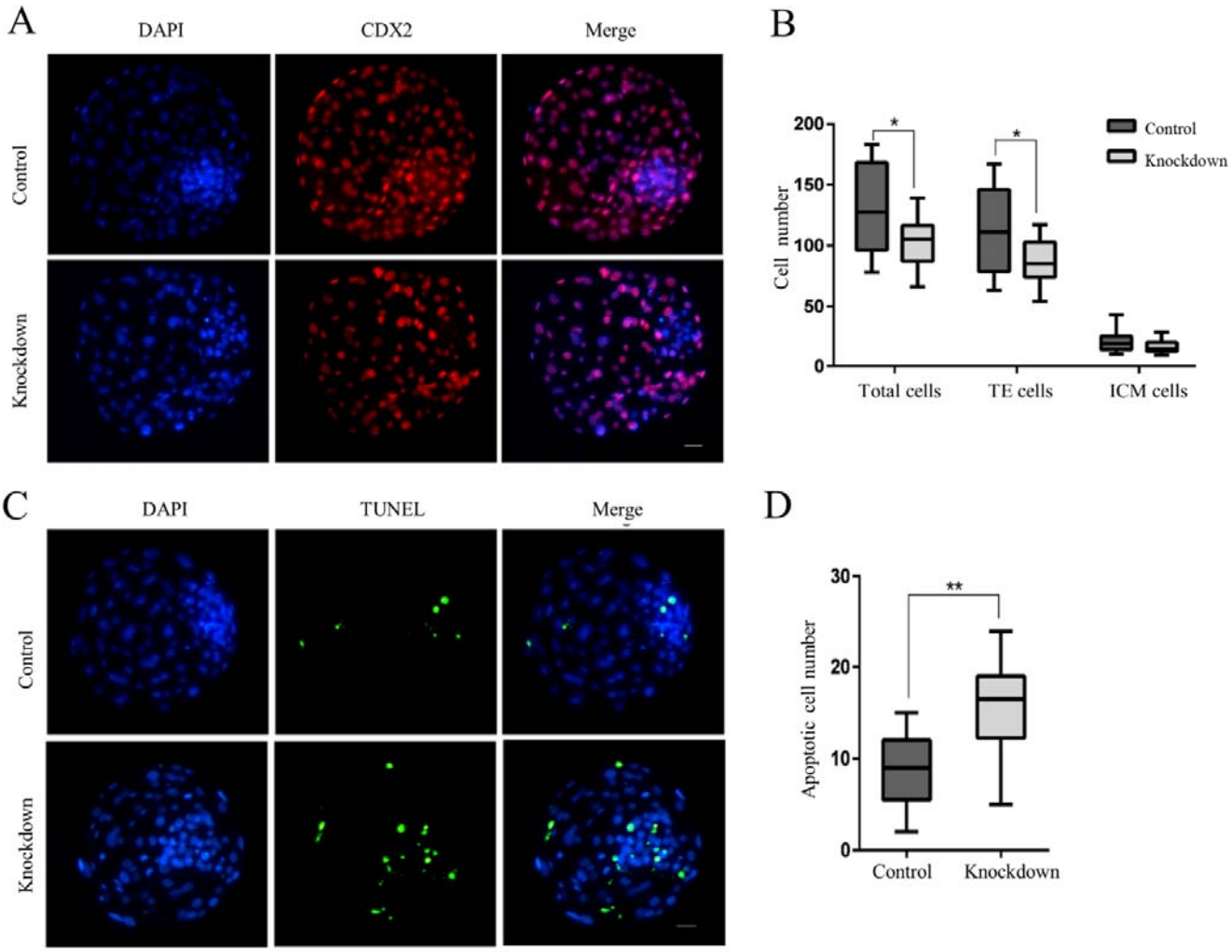

695

696 **Fig.7**

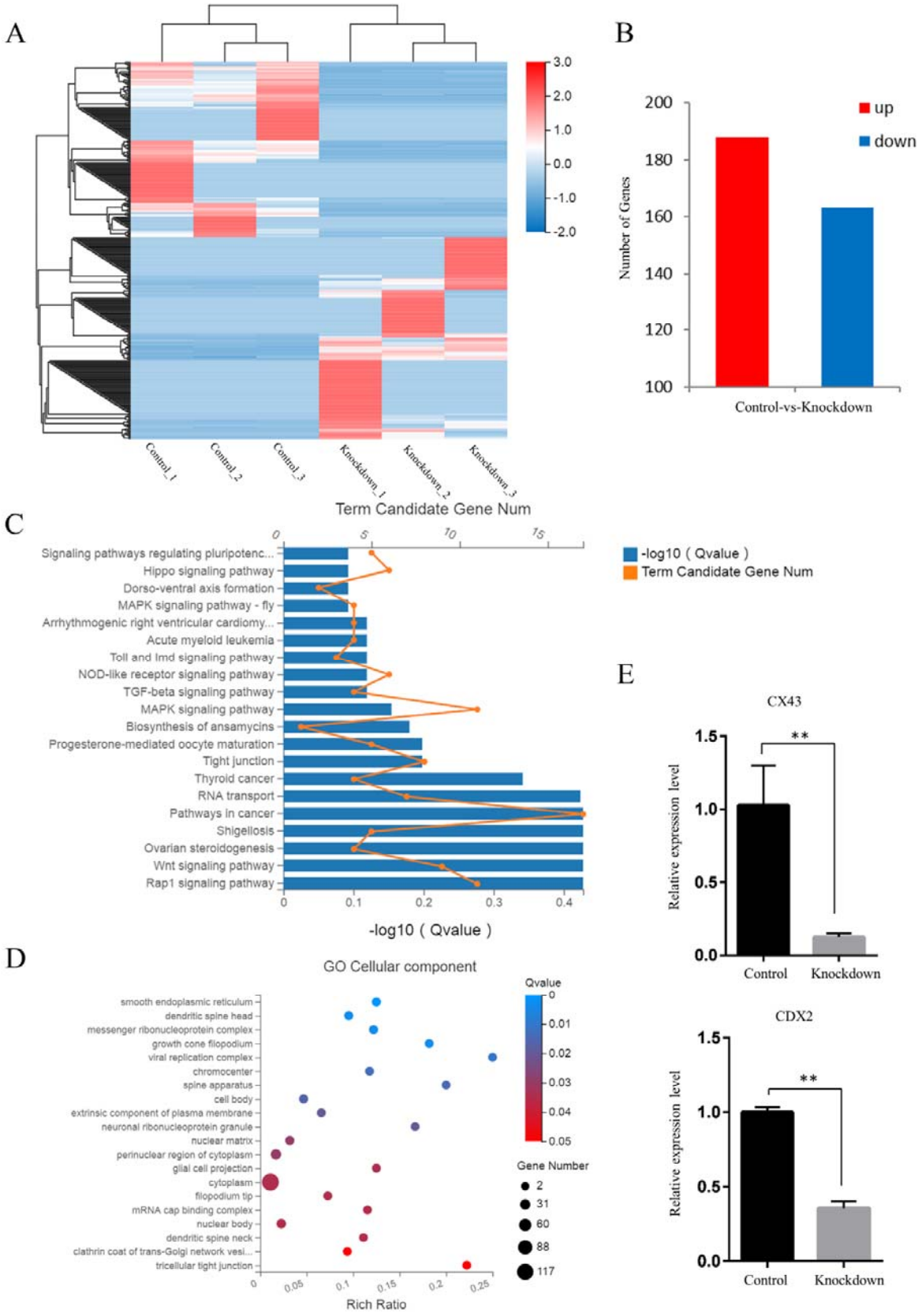

697 **Fig.S1**

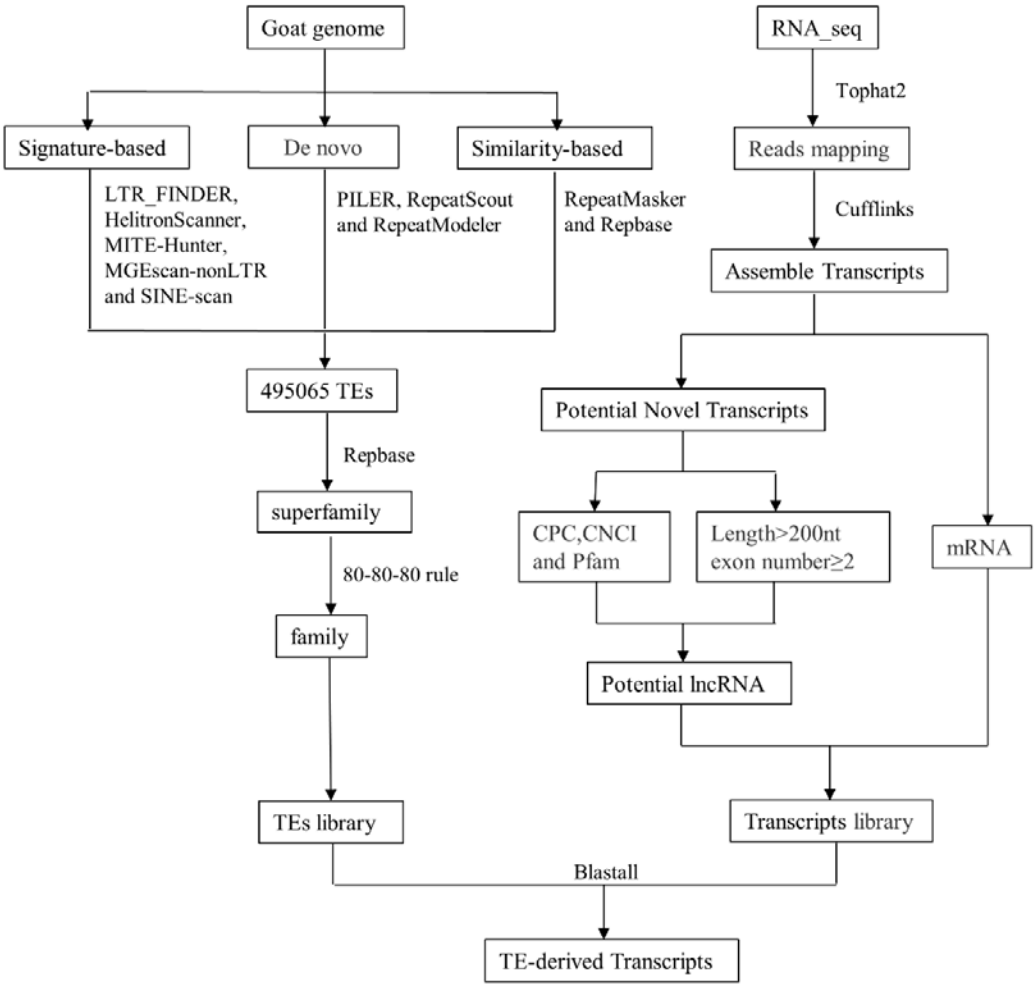

698

699

700 **Fig.S2**

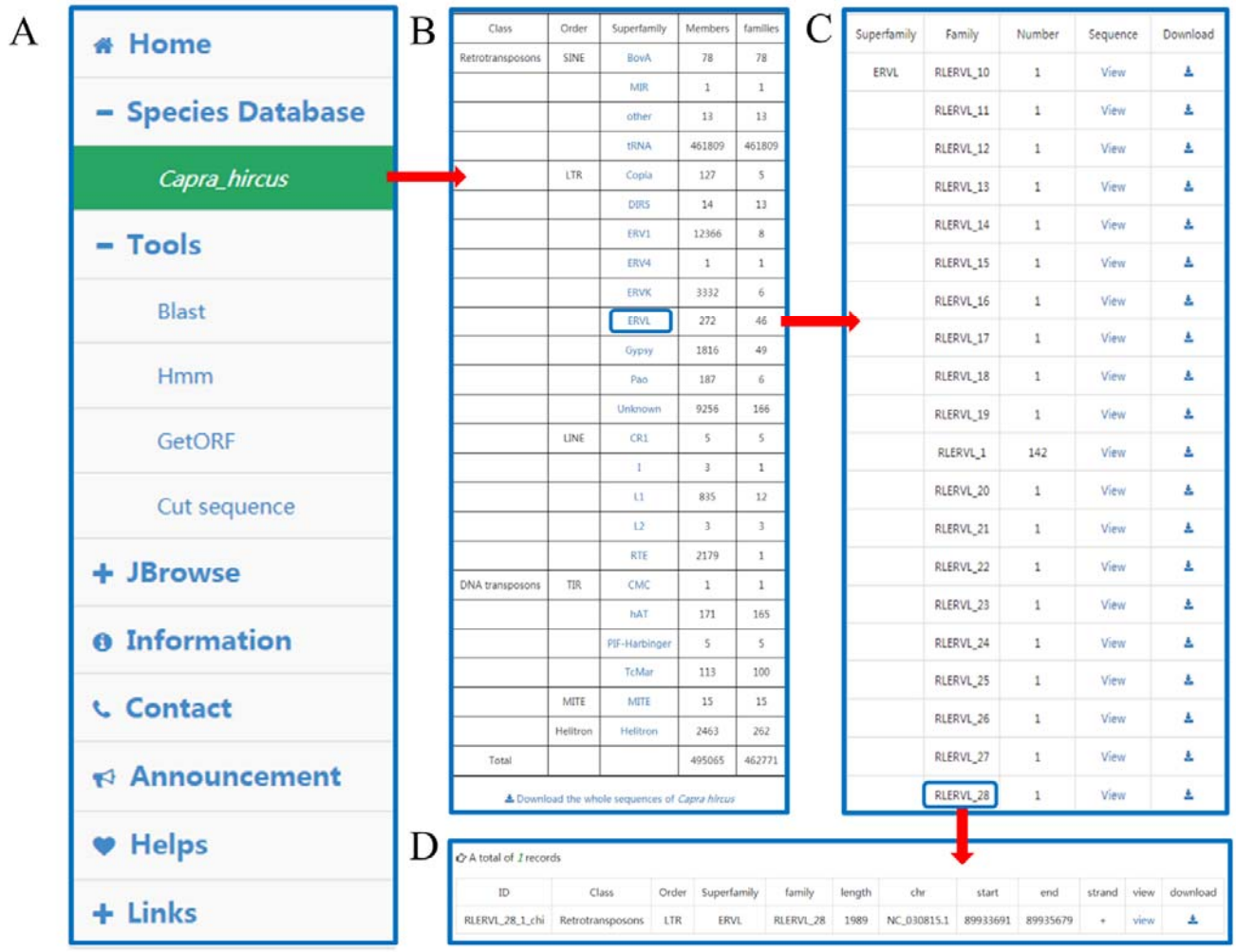

701

Fig.S3

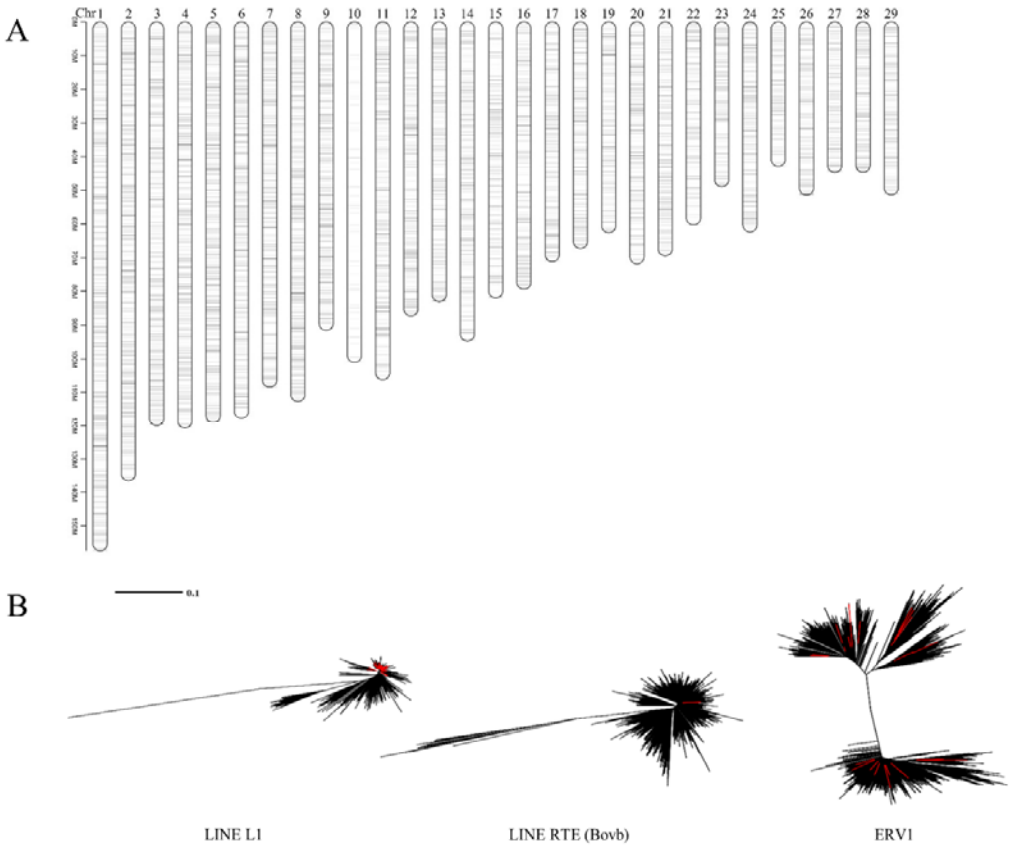

705 **Fig.S4**

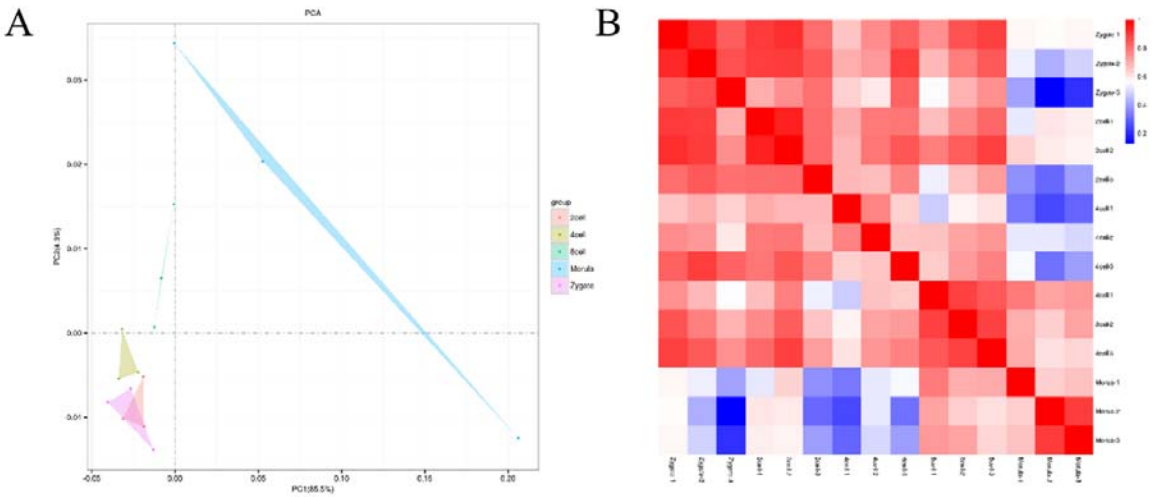

706

707

708 **Fig.S5**

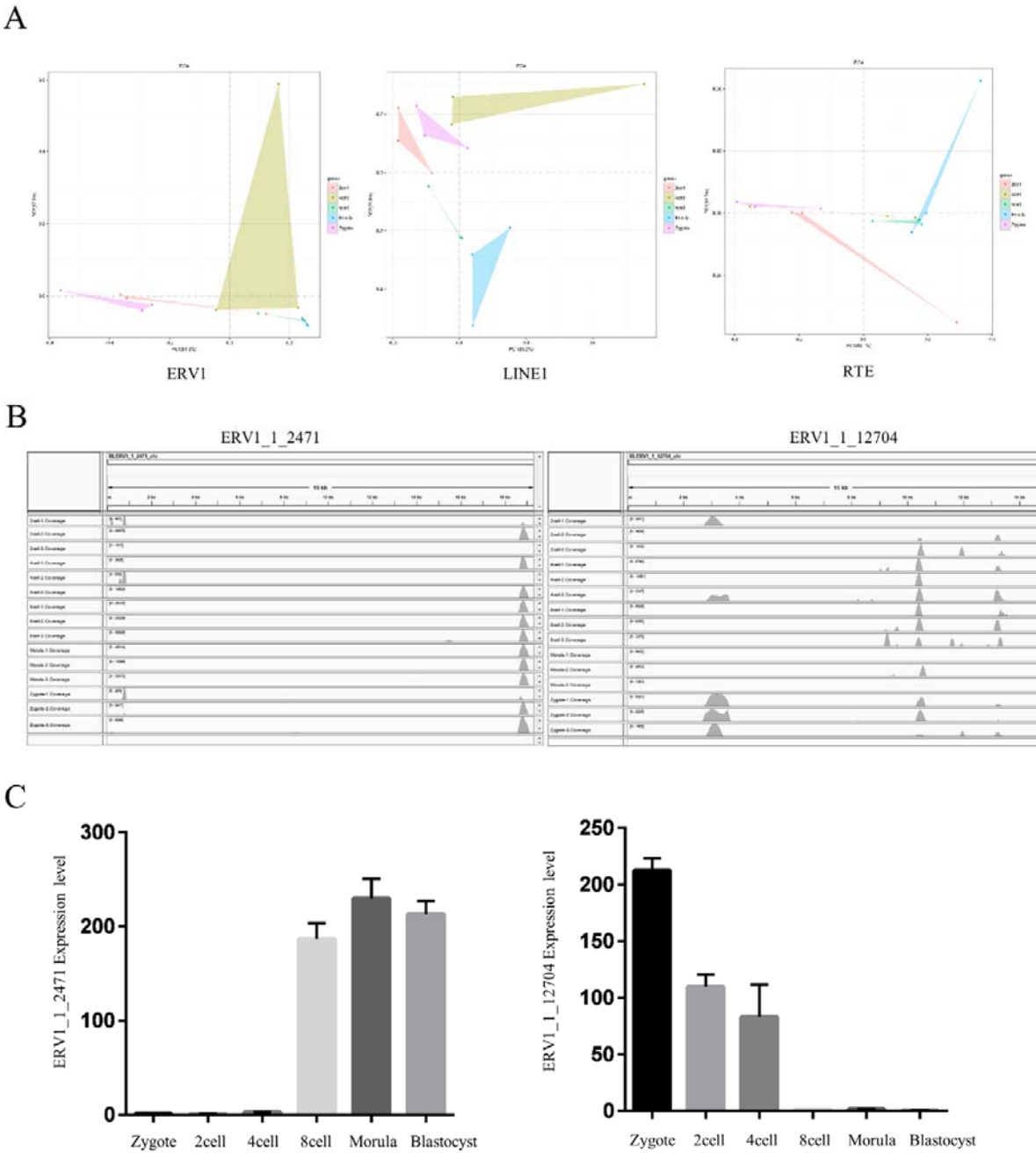

709

710 **Fig.S6**

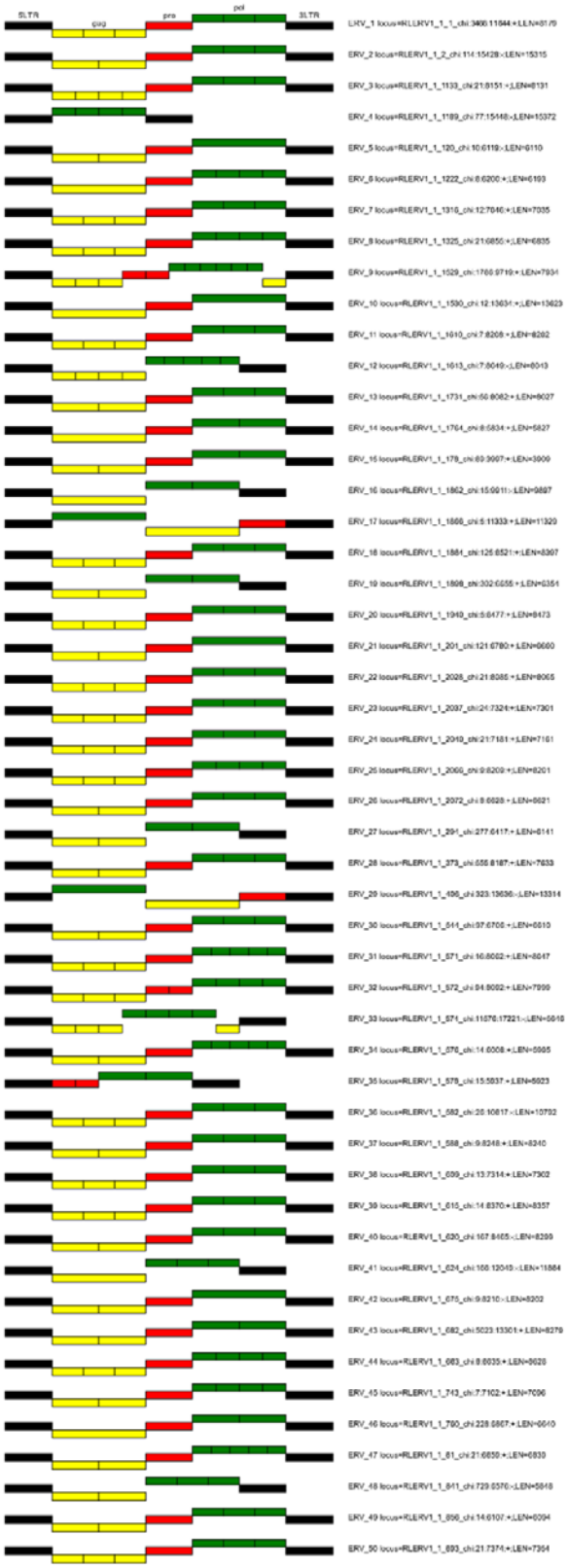

711